Status, issues and prospectives of lithium aluminates solid electrolyte including beta alumina in the form of film

Chen Chi[1,a,*]

[1]*School of Chemical Engineering and Pharmacy, Wuhan Institute of Technology, Wuhan, China*
[a]*15327326216@163.com*
[*]*Corresponding author*

Abstract: *Li-Beta alumina exhibited higher ionic conductivity than other lithium aluminate phases of $LiAl_5O_8$, $LiAlO_2$ and Li_5AlO_4 because of the special crystal structure having many conduction channels in c-plane. It is usually used as solid electrolyte in Battery. Compared with bulk and powder, Li-Beta alumina film takes advantages of decrease in area specific resistance, reduction of operating temperature, reduction of size/weight for battery and enhancement of battery cycle life. Laser chemical vapour deposition is used to achieve the first synthesis of Li-Beta alumina in form of film, which exhibits a high conductivity of 5.96 $S \cdot m^{-1} \cdot K$ at room temperature. In this process, the remained issue of Li loss is essential to be fixed for large-scale production.*

Keywords: *electrical conductivity; beta alumina; crystal structure; film*

1. Introduction

As people pay more attention to new energy technology, related metals and their compounds are extensively studied by researchers worldwide, such Li, Na, *etc*. The Li-Al-O system has several compounds of $LiAl_5O_8$, $LiAlO_2$ and Li_5AlO_4 and important Li-Beta alumina. Beta alumina exhibited very high ionic conductivity and is usually used as solid electrolyte in Battery, as depicted in Figure 1. Compared with Li_3N, LISICON and polymer-based lithium conductors, Li-Beta alumina has superior characteristic in ionic conduction.

Also $LiAl_5O_8$, $LiAlO_2$ and Li_5AlO_4 show more or less lithium ionic conductivity, which need more evidence to be applied to Li-battery so far. Of course they have lots of other properties of important. $LiAl_5O_8$ doped with rare-earth or transition ions is fine color emitting phosphors [1-3]. The dopant ions occupy tetrahedral sites in low-temperature α-phase or octahedral sites in high-temperature β-phase to produce emission spectra after excitation. $LiAl_5O_8$ (spinel) also has catalytic applications either as catalyst or as support because of excellent electron transfer ability, low surface acidity and higher catalytic activity than the traditional γ-Al_2O_3 support [4]. $LiAlO_2$ attracts increasing attention as a potential substrate for growing GaN semiconductor due to low lattice mismatch and removability [5]. It is also of interest as a solid tritium breeding material to produce tritium fuel by the nuclear reaction of Li (n, a)T in a fusion reactor, since $LiAlO_2$ shows high-temperature stability and good compatibility with structural materials under irradiation with neutrons [6]. Additionally, $LiAlO_2$ is thermochemically stable even at 973 K so that it is usually used as the support for the polymer electrolyte to form the diaphragm transporting CO_3^{2-} in molten carbonate fuel cells (MCFC) [7]. Aside from the stable $LiAl_5O_8$ and $LiAlO_2$, Li_5AlO_4 shows high reactivity with water (H_2O) and carbon dioxide (CO_2) in atmosphere because of high lithium content. Interaction between Li_5AlO_4 and H_2O causes the formation of LiOH, especially upon exposure to water vapor, which could lead to the humidity dependence of its conductivity. Therefore, Li_5AlO_4 is deemed to be a suitable material for humidity sensor [8, 9]. Li_5AlO_4 also has high capacity of CO_2 absorption, which makes it a promising carbon dioxide captor [10]. For the amorphous Li-Al-O materials, ionic conduction was exhibited with low lithium content (Li/Al molar ratio less than 0.2).

For the application of them in Li-ion battery, the form of film takes advantages of decrease in area specific resistance, reduction of operating temperature, reduction of size/weight for battery and enhancement of battery cycle life, as shown in Figure 2. However, it is extremely difficult to synthesize their films due to high saturated vapor pressure of lithium. So it is necessary to discuss the current

situation, problem, and future development of these Li-ionic electrolyte films and attempt to find a solution, especially for Li-Beta alumina.
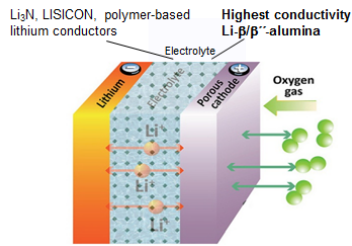

Figure 1: Schematic of Li- battery

Figure 2: Example of film battery

2. Prepation methods

Li-Al-O compounds in the forms of bulk and powder have been fabricated by solid state sintering, combustion and sol-gel methods. But only a few studies on the preparation of $LiAl_5O_8$ and amorphous lithium aluminate films were reported by using rf-magnetron sputtering, atomic layer deposition (ALD) and sol-gel methods. Significantly, there is no report on preparation of Li-Beta alumina film, which illustrates the complexity and difficulty for fabrication of lithium aluminate ceramics in the form of film. As we know, lots of processes, such as chemical vapor deposition (CVD), atomic layer deposition (ALD), physical vapor deposition (PLD) and tape casting (TP), can be used to achieve the preparation of various films including Li_2O, Al_2O_3 and $BaTi_2O_5$, *etc*. Then, we try to use these methods to synthesize Li-Beta alumina film, resulting in no detection of Li in final products. This could be explained by the high crystalline temperature of Li-Beta alumina and high saturated vapor pressure of lithium at elevated temperature. Obviously, high temperature is a hinder for preparing lithium aluminate films including Beta alumina. Consequently, attempting to introduce laser or plasma to activate the reactants may decrease crystalline temperature of these films.

Laser chemical vapor deposition (laser CVD) is a deposition technique for films of various materials by introducing activated field with laser irradiation for chemical reaction. A cold-wall chamber was constructed as the main part of laser CVD setup. A continuous wave laser (Diode or YAG) was employed. Precursors were evaporated in the furnace and their vapors were transported to the reaction region (substrate) by Ar carrier gas. Before deposition, the substrate was preliminarily pre-heated and irradiated by the laser through a quartz window at an incident angle of 45°. The chemical reaction on the substrate surface was thus activated greatly, which decreased the preparation temperature and accelerated the deposition of films, as shown in Figure 3.
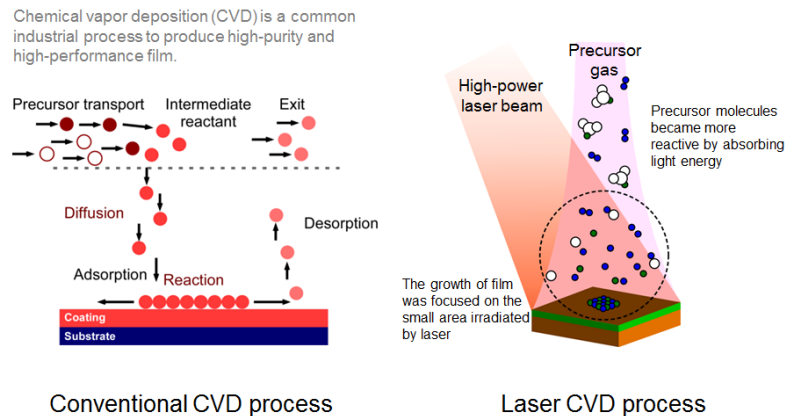

Figure 3: Comparison of conventional CVD process with laser-assisted CVD process

The parameters of deposition temperature (T_{dep}), laser power (P_L), molar ratio of Li/Al ($R_{Li/Al}$) and total pressure (P_{tot}) are mutually influenced in laser CVD. Figure 4 shows the effects of P_L and $R_{Li/Al}$ on T_{dep}. The T_{dep} linearly increased with increasing P_L and decreased with increasing $R_{Li/Al}$. The increase of $R_{Li/Al}$ would have caused a rise in concentration of precursor vapors in chamber; thus more heat radiation could be accompanied at higher $R_{Li/Al}$, resulting in the decrease in T_{dep}.
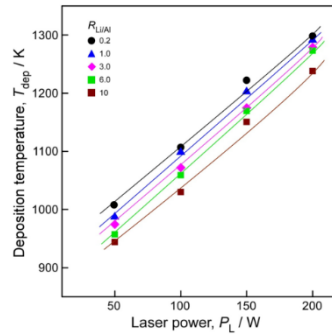
Figure 4: Effects of P_L (laser power) and $R_{Li/Al}$ (molar ratio of Li/Al) on T_{dep} (deposition temperature).

Figure 5 shows the effects of P_{tot} and $R_{Li/Al}$ on T_{dep} at P_L=150 W. The T_{dep} decreased with increasing P_{tot} and $R_{Li/Al}$. At higher P_{tot} or $R_{Li/Al}$, a higher concentration of precursors in gas phase existed in the chamber, causing more heat radiation from laser energy. That could lower the T_{dep} in reaction area. With decreasing P_{tot}, the influence of $R_{Li/Al}$ on T_{dep} became more notable.
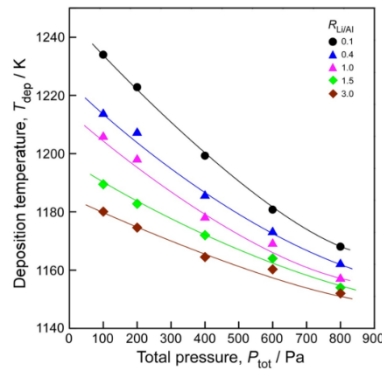

Figure 5: Effects of P_{tot} (total pressure) and $R_{Li/Al}$ (molar ratio of Li/Al) on T_{dep} (deposition temperature).

Figure 6 shows the ratio $R_{Li/Al}$ as a function of T_{Li} at T_{Al} = 443 K. The $R_{Li/Al}$ was estimated from the evaporated amounts of Al and Li precursors. By increasing T_{Li} from 483 to 553 K, the $R_{Li/Al}$ approximately increased from 0.1 to 10.
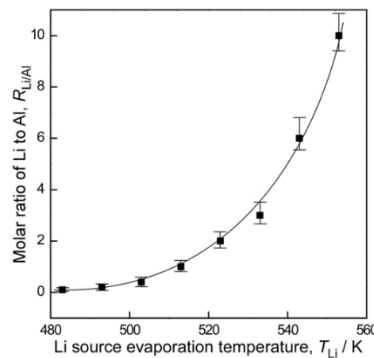

Figure 6: Effect of T_{Li} (evaporation temperature of Li precursor) on $R_{Li/Al}$ (molar ratio of Li/Al).

3. Crystal structures of Beta alumina and other lihitum aluminate compounds

Beta alumina group can be subdivided into those members containing a twofold screw axis in unit cell and those containing a threefold screw axis in unit cell. The archetypes of the two subgroups are designated β-alumina (twofold) and β"-alumina (threefold), respectively. Both of Li-β-alumina and Li-β"-alumina are characterized by structures composed of alternating slabs of closely-packed oxides (AlO_4, AlO_6) and loosely-packed layers with a low atom density containing mobile Li ions. Al^{3+} cations

occupy both octahedral and tetrahedral interstices in the closely-packed slabs, forming a dense spinel block to prevent Li ions moving along c-axis. The loosely-packed layer supplies enough space for Li ions to move and is therefore named conduction plane. Li-β-alumina contains a mirror plane through the layer of mobile Li ions in the hexagonal unit cell, as shown in Figure 7.
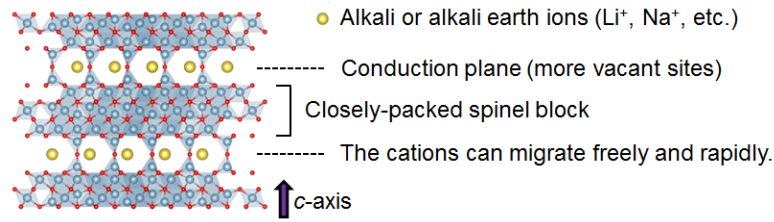

Figure 7: Crystal structure of Li-β-alumina.

The crystal structure of α-LiAl$_5$O$_8$ is an inverse spinel with a cubic lattice (space group: $P4332$, lattice constant: $a = 0.7908$ nm), as shown in Figure 8 (a). The Li atoms and half of the Al atoms form six-coordinated octahedra sharing their edges. The other Al atoms form four-coordinated tetrahedra sharing corners of the octahedra. The phase of α-LiAl$_5$O$_8$ with a Li-poor and Al-rich composition is situated next to Li–β-alumina in the phase diagram of the Al$_2$O$_3$–Li$_2$O system. Among the many polymorphs of alumina, γ-alumina has a defective spinel, as shown in Figure 8 (b) where Al atoms at tetrahedral and octahedral sites are designated as Al1 and Al2, respectively. The occupancy of the octahedral Al2 site is 0.83 to satisfy the Al$_2$O$_3$ stoichiometry in a spinel cubic cell. The crystal structure of α-LiAl$_5$O$_8$ can be understood as a derivative form of γ-Al$_2$O$_3$ with substitution of the Li-centered octahedra for a quarter of the Al2-centered ones.
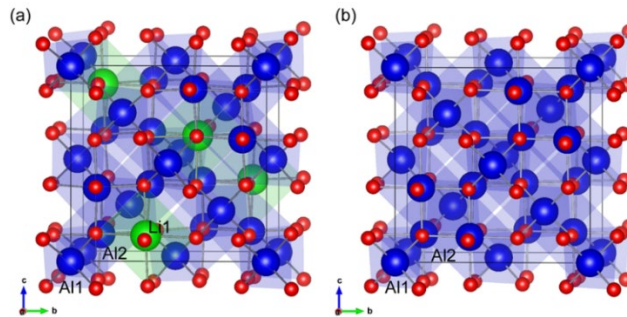

Figure 8: Crystal structures of α-LiAl$_5$O$_8$ (a) and γ-alumina (b).

LiAlO$_2$ has two types of structure, α: hexagonal caswellsilverite (NaCrS$_2$)-type and γ: tetragonal wurtzite-type. γ-LiAlO$_2$ has a wurtzite structure in a tetragonal cell ($P4_12_12$; $a = 0.517$ nm and $c = 0.6295$ nm), which is composed of Al- and Li-centered tetrahedral, as shown in Figure 9. Each tetrahedron shares one of its edges with another tetrahedron of a different type, and each vertex of every tetrahedron is shared with two additional tetrahedra. The edge-sharing couples of Al- and Li-centered tetrahedra are aligned on (00l) planes. This directional alignment of the edge-sharing couples of tetrahedra could be associated with the preferred (001) orientation in the γ-LiAlO$_2$ film.

Li$_5$AlO$_4$ also has two types of structure, α: antifluorite and β: antifluorite with greater disorder of the cations and vacancies in the tetrahedral sites. β-Li$_5$AlO$_4$ has a defective antifluorite structure ($Pmmn$; $a = 0.642$ nm, $b = 0.6302$ nm, and $c = 0.462$ nm), which is derivative form of the cubic antifluorite structure of Li$_2$O. Figure 10 depicts schematics of the crystal structures of (a) β-Li$_5$AlO$_4$ and (b) Li$_2$O. In the cubic antifluorite structure of Li$_2$O, Li-centered tetrahedra with O atoms occupying the face-centered sites form an edge-sharing network. Compared with the crystal structures of Li$_2$O shown in a different view in Figure 10 (c), the structure of β-Li$_5$AlO$_4$ is analogous to that of Li$_2$O. The substitution of Al ions by Li ions at the center of the tetrahedra results in the formation of tetrahedral anion vacancies to satisfy charge compensation, accompanied by orthorhombic distortion from the cubic symmetry.
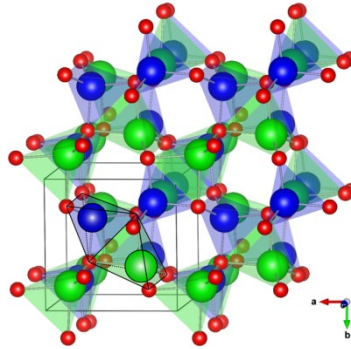
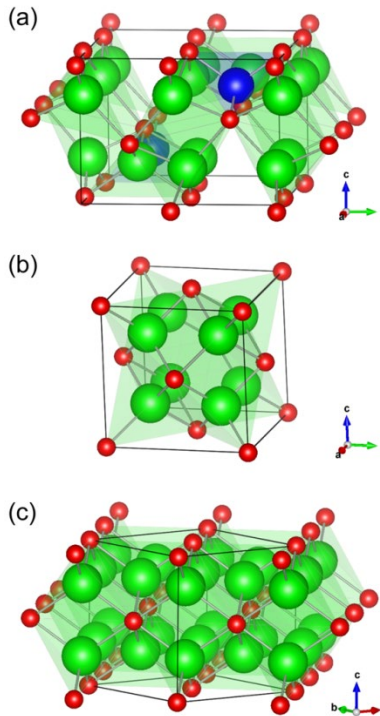*Figure 9: Crystal structure of γ-LiAlO₂ viewed along approximately normal to c-plane.*

Figure 10: Crystal structures of β-Li₅AlO₄ (a) and Li₂O (b, c).
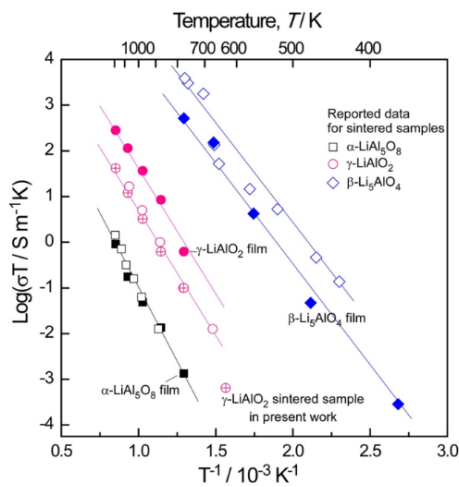
4. Electrical properties of Li-Al-O films

Figure 11: Comparison of electrical conductivities of α-LiAl₅O₈, γ-LiAlO₂, and β-Li₅AlO₄ films.

The electrical conductivities of α-LiAl$_5$O$_8$, γ-LiAlO$_2$, and β-Li$_5$AlO$_4$ films were summarized in Figure 11. The dependence of logarithm of σT on inverse of temperature ($1000/T$) for Li-Al-O films showed a typical Arrhenius behavior. α-LiAl$_5$O$_8$ film almost had the same electrical conductivity as the reported data for its sintered sample. γ-LiAlO$_2$ film showed higher electrical conductivity than its sintered sample and α-LiAl$_5$O$_8$ film. β-Li$_5$AlO$_4$ film presented the highest electrical conductivity among the deposited Li-Al-O films, reaching 515 S·m^{-1}·K at 773 K. Although Li-rich film of Li$_5$AlO$_4$ exhibited very high ion conduction at high temperature, its electrical conductivity at room temperature is low and unable to replace Li-Beta alumina. Even at room temperature (298 K) Li-Beta alumina film has a σT value of 5.96 S·m^{-1}·K while it shows much higher lithium ion conductivity than other solid electrolytes at any prevailing temperatures. To date, the only problem to be solved for the application of Li-Beta alumina film electrolyte is saving the huge consumption of lithium-containing precursor, which is deemed to compensate the loss of Li at high synthesis temperature due to high vapor pressure of Li.

5. Conclusions

Lithium aluminate materials are used in numerous fields and their films exhibit superior characteristics, especially in electrical conduction. As solid electrolyte, Li-Beta alumina is the most suitable one of them due to loose channel of conduction c-plane in its crystal structure where lithium ions can move freely and rapidly. Furthermore, Li-Beta alumina in form of film can decrease resistance, reduce operating temperature and enhance battery cycle life. Although the preparation of Li-Beta alumina film is quite complex and difficult, laser or plasma used together with chemical vapor deposition process is able to pre-activate the gaseous precursor, which decrease synthesis temperature and avoid excessive loss of Li. In our previous work, laser-assisted CVD has been used to synthesize various ceramic films such as Al$_2$O$_3$ and CeO$_2$. Also laser CVD process is successful for preparation of Li-Beta alumina film, in which the remained issue we need to solve is saving raw materials. This could be accomplished throughout improvement of whole device and process optimization.

Acknowledgements

References

[1] Ishihara T, Tanaka K, Hirao K, Soga N, John D. Mackenzie. Optical properties of LiAl$_5$O$_8$:Fe^{3+} film prepared by the sol-gel method. Sol-Gel Optics III, 1994, 2288: 668-677.

[2] T. Abritta, F. de Souza Barros. Luminescence and photoacoustic measurements of LiAl$_5$O$_8$: Fe^{3+}. J. Lumin., 1988, 40: 187-188.

[3] J.M. Neto, T. Abritta, F. de S. Barros, N.T. Melamed. A comparative study of the optical properties of Fe3+ in ordered LiGa5O8 and LiAl5O8. J. Lumin., 1981, 22: 109-120.

[4] Y. Ge, Y. Dong, S. Wang, Y. Zhao, J. Lv, X. Ma. Influence of crystalline phase of Li-Al-O oxides on the activity of Wacker-type catalysts in dimethyl carbonate synthesis. Front. Chem. Sci. Eng., 2012, 6: 415-422.

[5] X. He, G. Meng, X. Zhu, M. Kong. Synthesis of vertically oriented GaN nanowires on a LiAlO2 substrate via chemical vapor deposition. Nano Res., 2009, 2: 321-326.

[6] F. Botter, B. Rasneur, E. Roth. Irradiation behaviour of a tritium breeding material, γ-LiAlO$_2$ results of two in-pile experiments: ALICE I and ALICE II. J. Nucl. Mater, 1988, 160: 48-57.

[7] A.N. Webb, J.W.B. Mather, R.M. Suggitt. Studies of the Molten Carbonate Electrolyte Fuel Cell. J. Electrochem. Soc., 1965, 112: 1059-1063.

[8] I.D. Raistrick, C. Ho, R.A. Huggins. Lithium ion conduction in Li$_5$Al0$_4$, Li$_5$GaO$_4$ and Li$_6$ZnO$_4$. Materials Research Bulletin, 1976, 11: 953-957.

[9] R.T. Johnson Jr, R.M. Biefeld. Ionic conductivity of Li$_5$AlO$_4$ and Li$_5$GaO$_4$ in moist air environments: Potential humidity sensors. Mater. Res. Bull., 1979, 14: 537-542.

[10] T. Ávalos-Rendón, J. Casa-Madrid, H. Pfeiffer. Thermochemical Capture of Carbon Dioxide on Lithium Aluminates (LiAlO$_2$ and Li$_5$AlO$_4$): A New Option for the CO$_2$ Absorption. J. Phys. Chem. A, 2009, 113: 6919-6923.